Texture Development of Ti-Zr-Nb Alloy Under High-Temperature Deformation

Makoto Hasegawa[1], Pramote Thirathipviwat[1], Equo Kobayashi[2], Osamu Umezawa[1] and Hiroshi Fukutomi[3, 4]

[1]*Division of Systems Research, Faculty of Engineering, Yokohama National University, Yokohama 240-8501, Japan*
[2]*Department of Materials Science and Engineering, School of Materials and Chemical Technology, Tokyo Institute of Technology, Tokyo 152-8552, Japan*
[3]*Professor Emeritus, Yokohama National University, Yokohama 240-8501, Japan*
[4]*Specially Appointed Professor, Osaka University, Osaka 565-0871, Japan*

Ti-46Zr-8Nb (mol%) alloy was subjected to uniaxial compressive deformation under various deformation conditions to investigate microstructure and texture evolution. The possibility of the occurrence of preferential dynamic grain growth was also researched. Uniaxial compression tests were carried out at various temperatures ranging from 473 K to 1473 K with true strain rates from 1×10^{-2} to 1×10^{-4} s^{-1} up to a true strain of -1.0. The work-softening type true stress-true strain curves were observed in the deformation conditions where the temperature was higher than 873 K. When the conditions were lower than 873 K, work-hardening type true stress-true strain curves were detected. The main component of the texture was {001} which indicates the formation of {001} fiber texture in the deformation conditions in which the temperature was higher than 873 K. This texture formation is considered due to the occurrence of the preferential dynamic grain growth.

Keywords: *high-temperature deformation, texture, orientation control, preferential dynamic grain growth*

1. Introduction

The β-type Ti alloy is lightweight and has excellent mechanical properties. It also exhibits excellent biocompatibility such as corrosion resistance and hypoallergenic. Therefore, it has been applied as an implant material to replace hard tissues such as bone. The β-Ti alloy exhibits a relatively low Young's modulus ranging from 60 to 80 GPa [1)]. However, its modulus is higher than that of bone, which has Young's modulus of about 10 to 30 GPa. Thus, inhibition of bone formation by stress shielding has become a problem. A material having Young's modulus close to that of bone is required. The β-Ti alloy has a bcc lattice, and it is known that Young's modulus of the bcc lattice varies depending on the crystal orientation [2)]. Generally, Young's modulus is highest at <111> orientation and lowest at <100> orientation. It is reported that Young's modulus of <100> orientation in a single crystal of Ti-46Zr-8Nb (mol%) alloy is ~36 GPa [3)]. Therefore, the texture control along <100> orientation is effective for lowering Young's modulus. The texture formation of solid solution alloy under high-temperature plane strain compression has been investigated so far. In Fe-Si alloys, grains having a small Taylor factor and a stable orientation for a given deformation mode grow preferentially. It is reported that a rotated cube texture where <100> orientation is tilted about 45° from the rolling direction has formed [4)]. This grain growth behavior is so-called preferential dynamic grain growth [5)]. Therefore, it has a possibility that the β-Ti alloy develops a rotated cube texture. However, it is not clear whether preferential dynamic grain growth occurs in β-Ti alloys. Furthermore, the deformation conditions under which the texture develops the most are not clear. In this study, Ti-46Zr-8Nb (mol%) alloy was subjected to high-temperature uniaxial compressive deformation under various deformation conditions. The conditions under which the texture develops due to preferential dynamic grain growth were investigated experimentally.

2. Experiment

2.1 Materials and uniaxial compression tests

Ti-46Zr-8Nb (mol%) alloy was used as the testing material. Bars of the alloy with a cross-section of 25 × 25 mm were produced by groove rolling under high temperature. Then, the bars were rolled up to 50% at room temperature. Cylindrical specimens with a diameter of 8 mm and a height of 12 mm were prepared by machining with a lathe. At this time, grooves with a depth of about 0.1 mm were cut concentrically at intervals of 0.5 mm on the bottom surface of the specimens. Through this processing, the lubricant (BN) is retained in the grooves during compressive deformation to ensure smooth lubrication between specimen and punch. The specimens were heat treated in a vacuum at 1073 K for 1.8 ks.

Uniaxial compression tests under high temperature were conducted by a servo-hydraulic testing machine with a high-frequency induction heating furnace. The specimen was heated in a vacuum at a heating rate of 10 K/s to the testing temperature and held there for 0.9 ks. Then, tests were performed at temperatures of 473 K to 1473 K and true strain rates of 1×10^{-2} to 1×10^{-4} s^{-1}. After uniaxial compression up to a true strain of -1.0, the specimen was immediately cooled by blowing nitrogen gas to freeze the microstructure.

2.2 Microstructure observation

After the compression processes, mid-plane section and cross-section specimens were prepared by mechanical and chemical mechanical polishing. Microstructures were observed by an optical microscope (OM) and a scanning electron microscope (SEM). Measurement of the local crystal orientations of the uniaxially compressed specimens

was conducted by the electron backscattered diffraction (EBSD) technique. The texture was characterized by using the Schulz reflection method, with Cu-Kα radiation filtered by a monochromator. Mid-plane section of the specimen was measured. From the pole figures obtained, the orientation distribution function (ODF) was calculated by the arbitrarily defined cell method [6]. The main component and sharpness of the texture, which corresponds to the position and value of the maximum pole density, were determined from the normalized pole figure and inverse pole figure derived from the ODF. The volume fractions for the regions aligned within 15° of the main component were calculated.

3. Results and Discussion

3.1 Microstructure before deformation

Fig. 1 shows the microstructure and X-ray diffraction pattern obtained from the Ti-46Zr-8Nb (mol%) alloy after heat treatment. The average grain size of the microstructure was 149 μm. From Fig. 1(b), all peaks are signals from the β phase. Signals from other phases were not detected. This means that the alloy is β single phase material.

3.2 Deformation behavior

Fig. 2 shows true stress–true strain curves of Ti-46Zr-8Nb (mol%) alloy deformed uniaxially under various true strain rates at 1173 K up to a true strain of -1.0. The curves are of the work softening type. The flow stress reaches a maximum at an early stage of deformation and

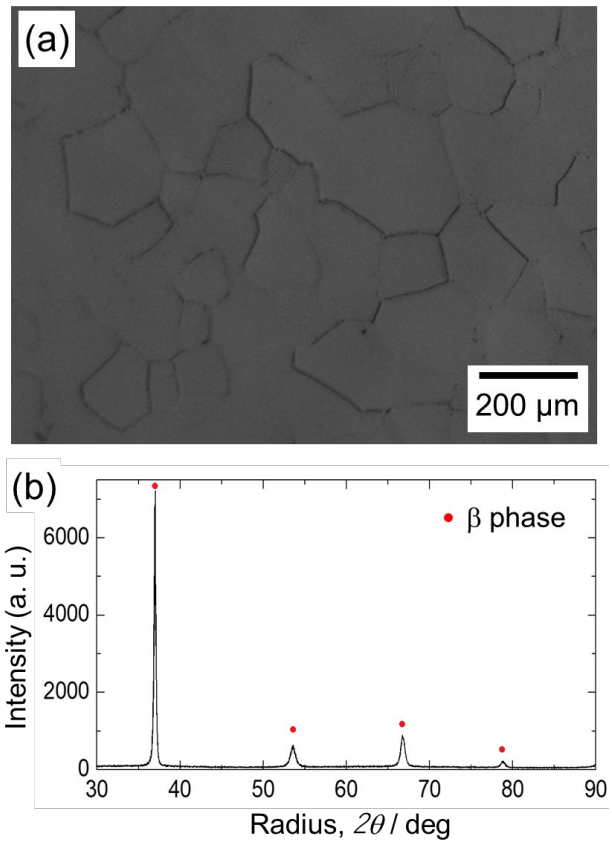

Fig. 1 (a) Microstructure and (b) X-ray diffraction pattern of the Ti-46Zr-8Nb (mol%) alloy after heat treatment at 1073 K for 1.8 ks

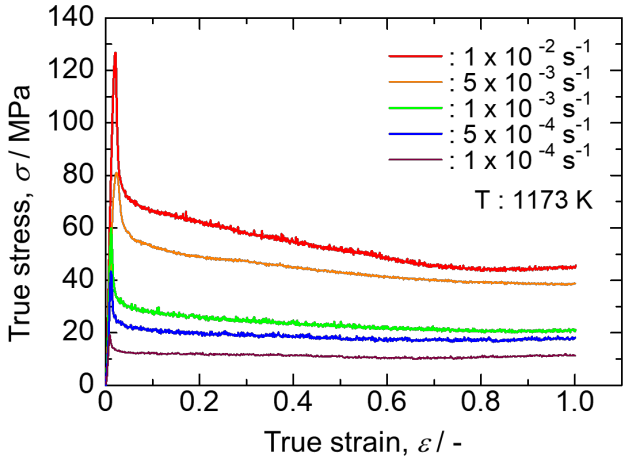

Fig. 2 True stress–true strain curves of the Ti-46Zr-8Nb (mol%) alloy obtained by compression test at 1173 K under various true strain rates. The compression was conducted up to a true strain of -1.0

then decreases with further deformation. The steep increase and subsequent decrease in stress could be seen. Work softening of the true stress–true strain curves could be observed at a temperature higher than 873 K. At a temperature lower than 873 K, work hardening was observed. In the true stress–true strain curves indicating work softening, the stress when the true strain was -0.5 was defined as the flow stress, σ_s. Increasing the deformation temperature and decreasing the true strain rate decreases the flow stress, σ_s, of the true stress–true strain curve. During high-temperature deformation of the metals and alloys, the flow stress is usually affected by the temperature and the true strain rate. The relationship between these parameters can be expressed by using the Garofalo equation [8] and the Zemer-Hollomon parameter, Z, as

$$Z = \dot{\varepsilon} \cdot \exp(Q/RT) = A \cdot \{\sinh(\alpha \cdot \sigma_s)\}^n \qquad (1)$$

where n, Q, and R are the stress exponent, the apparent activation energy for high-temperature deformation, and the gas constant, respectively, and A and α are material constants. The Q and n were calculated as Q=137 kJ/mol and n=3.0. It is known that the self-diffusion energy of β-Ti, β-Zr, and Nb are 131 kJ/mol [9], 90 kJ/mol [10], and 397 kJ/mol [11], respectively. The obtained Q is close to the self-diffusion energy of β-Ti. Furthermore, the value of n was the value of a solid solution type.

There are two deformation characteristics detected in the Ti-46Zr-8Nb (mol%) alloy.

1) At the deformation temperature higher than 873 K, work softening type true stress–true strain curves having a steep increase and subsequent decrease in stress are available.
2) Zemer-Hollomon parameter could be described as a function of flow stress.

These behaviors are similar to the high-temperature deformation characteristics of the Al-Mg solid solution alloys [7]. Therefore, the work softening behavior in Fig. 2 is considered to have a high possibility of a high temperature-yielding phenomenon.

3.3 Microstructure and texture after deformation

Microstructure after high-temperature deformation indicates undulation of the grain boundary due to the grain boundary migration. In addition, it seems that the degree of the grain boundary undulation during grain boundary migration increases with the increase in compressive strain during high-temperature deformation. Grains having {001} orientation parallel to the compression plane show larger grain size compared to the grains having other orientation.

Fig. 3 shows inverse pole figures after uniaxial compression at low and high temperatures. Inverse pole figures show the pole density distributions in the compression plane. The mean pole density is used as a unit. As shown in Fig. 3 (a), under deformation conditions where the deformation temperature is 473 K, the main component existed in {111} indicating the formation of {111} fiber texture. Regarding Fig. 3 (b), under deformation conditions where the deformation temperature is 1123 K, the main component exists in {001} indicating the formation of {001} fiber texture.

It is reported that grains having a small Taylor factor and a stable orientation for a given deformation mode grow preferentially. This grain growth behavior is so-called preferential dynamic grain growth. Characteristics of the microstructure development, grain boundary migration and undulation, and the formed texture shown above in our research indicate nearly the same behavior and characteristics which was already reported in the Fe-Si alloy [12] and Ti-Nb alloy [13]. Therefore, it seems that the Ti-46Zr-8Nb (mol%) alloy may also show preferential dynamic grain growth behavior under high-temperature deformation.

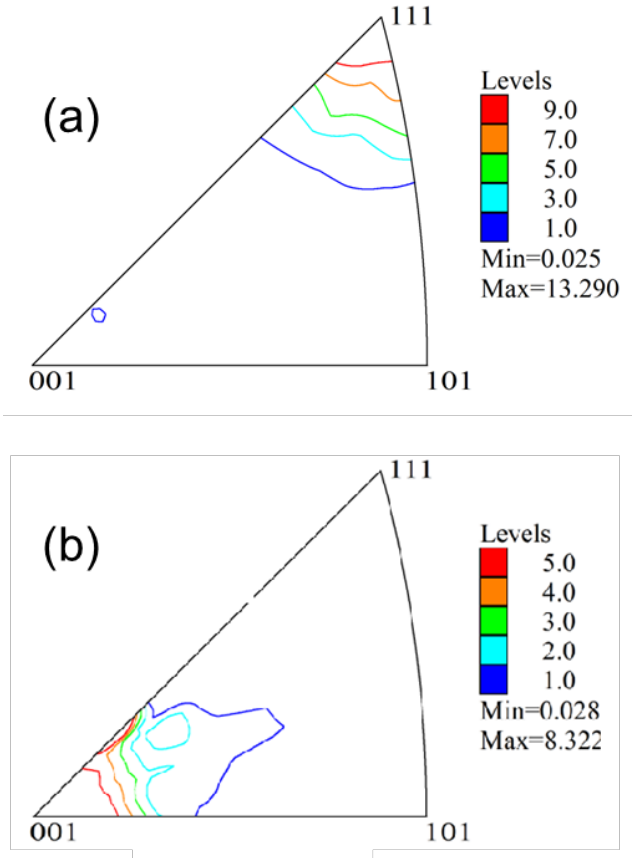

Fig. 3 Inverse pole figures of the Ti-46Zr-8Nb (mol%) alloy showing the distribution of pole densities of the compression plane. The mean pole density was used as a unit. The compression was conducted under various deformation conditions up to a true strain of -1.0. (a) T=473 K, $\dot{\varepsilon}$=1.0x10^{-3}s^{-1}, and (b) T=1123 K , $\dot{\varepsilon}$ =1.0x10^{-3}s^{-1}.

4. Conclusions

The evolution of microstructure and texture in Ti-46Zr-8Nb (mol%) alloy was examined under high temperatures uniaxial compression. The major conclusions are summarized as follows.

1. In high-temperature uniaxial compression deformation, true stress–true strain curves of work softening type were obtained when the temperature was higher than 873 K. The steep increase and subsequent decrease of the stress have a high possibility of indicating high temperature-yielding phenomena.
2. The main component of the formed texture was {001}. This is independent of the deformation condition above 873 K. This texture formation is considered by the occurrence of the preferential dynamic grain growth.

Acknowledgments

This paper was supported by project No. CZ.02.1.01/0.0/0.0/17_049/ 0008441 “Innovative Therapeutic Methods of the Musculoskeletal System in Accident Surgery” as part of the Operational Program Research, Development and Education financed by the European Union and by the state budget of the Czech Republic.

References

1) M. Niinomi: Mater. Trans., 59 (2018) 1-13.
2) P. Wang, M. Todai and T. Nakano: J. Alloys Comp., 782 (2019) 667-671.
3) Y. Yokoyama, E. Kobayashi, Y. Kimura and T. Sato: Proc. Inter. Symp. EcoTopia Sci., (2015) 1025.
4) Y. Onuki, R. Hongo, K. Okayasu and H. Fukutomi: Acta Mater. 61 (2013) 1294-1302.
5) H. Fukutomi, K. Okayasu, Y. Onuki, M. Hasegawa, E. Kobayashi, B. Strnadel and O. Umezawa: Mater. Trans., 63(2022) 148-156.
6) K. Pawlik, J. Pospiech and K. Lücke: Text. Microstruct., 1418, (1991) 25-30.
7) R. Horiuchi, H. Yoshinaga and S. Hama: J. Japan Inst. Metals, 29 (1965) 85-92.
8) F. Garofalo: Trans. Metal. Soc. AIME, 227 (1963) 351-355.
9) J.F. Murdock, T. S. Lundy and E. E. Stansbury: Acta Metall., 12 (1964) 1033-1039.
10) T. S. Lundy and J. I. Federer: Oak Ridge Report (USA) ORNL-3339 (1962) 1-27.
11) D. Ablitzer: Phil. Mag. 35 (1977) 1239-1256.
12) Y. Onuki, K. Okayasu and H. Fukutomi: Tetsu-to-Hagané: 98 (2012) 177-183.
13) Y. Hayakawa and O. Unezawa: J. Alloys Comp., 871 (2021) 159603.